Activation of SF1 neurons in the ventromedial hypothalamus by DREADD technology increases insulin sensitivity in peripheral tissues

Eulalia A. Coutinho,[1,2] Shiki Okamoto,[1,2] Ayako Wendy Ishikawa,[2,3] Shigefumi Yokota,[1] Nobuhiro Wada,[4,5] Takahiro Hirabayashi,[4] Kumiko Saito,[1] Tatsuya Sato,[1] Kazuyo Takagi,[1,6] Chen-Chi Wang,[2,7] Kenta Kobayashi,[2,8] Yoshihiro Ogawa,[9,10,11] Seiji Shioda,[4] Yumiko Yoshimura,[2,3] Yasuhiko Minokoshi[1,2]

[1]Division of Endocrinology and Metabolism, Department of Homeostatic Regulation, National Institute for Physiological Sciences, National Institutes of Natural Sciences, Okazaki, Aichi 444-8585, Japan.

[2]Department of Physiological Sciences, School of Life Sciences, SOKENDAI (The Graduate University for Advanced Studies), Hayama, Kanagawa 240-0115, Japan.

[3]Division of Visual Information Processing, Department of Fundamental Neuroscience National Institute for Physiological Sciences, National Institutes of Natural Sciences, Okazaki, Aichi 444-8585, Japan.

[4]Global Research Center for Innovative Life Science, Hoshi University School of Pharmacy and Pharmaceutical Sciences, Tokyo 142-8501, Japan.

[5]Department of Diabetes and Metabolic Diseases, Graduate School of Medicine, The University of Tokyo, Tokyo 113-8655, Japan.

[6]Department of Human Life Science, Nagoya University of Economics, Inuyama, Aichi 484-8504, Japan.

[7]Center for Experimental Animals, National Institutes of Natural Sciences, Okazaki, Aichi 444-8585, Japan.

[8]Section of Viral Vector Development, Center for Genetic Analysis of Behavior, National Institute for Physiological Sciences, National Institutes of Natural Sciences, Okazaki, Aichi 444-8585, Japan.

[9]Department of Molecular Endocrinology and Metabolism, Graduate School of Medical and Dental Sciences, Tokyo Medical and Dental University, Tokyo 113-8510, Japan.

[10]Department of Medicine and Bioregulatory Science, Graduate School of Medical Sciences, Kyushu University, Fukuoka 812-8582, Japan.

Diabetes Publish Ahead of Print, published online July 3, 2017

[11]Japan Agency for Medical Research and Development, CREST (AMED-CREST), Tokyo 100-0004, Japan.

Short title: Activation of SF1 neurons by DREADD technology

Word count (main text): 5775

Number of figures: 6

Supplemental Material: Supplemental Figures 1 and 2, and Supplemental Table

Correspondence to: Yasuhiko Minokoshi, MD, PhD, Division of Endocrinology and Metabolism, Department of Homeostatic Regulation, National Institute for Physiological Sciences, National Institutes of Natural Sciences, 38 Nishigonaka, Myodaiji, Okazaki, Aichi 444-8585, Japan. Tel.: +81-564-55-7741. Fax: +81-564-55-7743. Email: minokosh@nips.ac.jp

ABSTRACT

The ventromedial hypothalamus (VMH) regulates glucose and energy metabolism in mammals. Optogenetic stimulation of VMH neurons that express steroidogenic factor 1 (SF1) induces hyperglycemia. However, leptin acting via the VMH stimulates whole-body glucose utilization and insulin sensitivity in some peripheral tissues, whereas this effect of leptin appears to be mediated by SF1 neurons. We examined the effects of activation of SF1 neurons with DREADD (designer receptors exclusively activated by designer drugs) technology. Activation of SF1 neurons by intraperitoneal injection of clozapine-*N*-oxide (CNO), a specific hM3Dq ligand, reduced food intake and increased energy expenditure in mice expressing hM3Dq in SF1 neurons. It also increased whole-body glucose utilization, and glucose uptake in red-type skeletal muscle, heart, and interscapular brown adipose tissue (BAT), as well as glucose production and glycogen phosphorylase *a* activity in the liver, thereby maintaining blood glucose levels. During hyperinsulinemic-euglycemic clamp, such activation of SF1 neurons increased insulin-induced glucose uptake in the same peripheral tissues and tended to enhance insulin-induced suppression of glucose production by suppressing gluconeogenic gene expression and glycogen phosphorylase *a* activity in the liver. DREADD technology is thus an important tool for studies of the role of the brain in regulation of insulin sensitivity in peripheral tissues.

The ventromedial hypothalamus (VMH) plays a key role in the control of energy homeostasis (1) and glucose metabolism (2, 3). Electrical stimulation of the VMH was thus found many years ago to increase glucose production by the liver (4). Expression of steroidogenic factor 1 (SF1), also known as adrenal 4-binding protein (AD4BP), defines a specific subset of VMH neurons (5-7). Genetic disruption of glutamate release from SF1 neurons in mice attenuated recovery from insulin-induced hypoglycemia, suggesting that glutamatergic SF1 neurons are responsible for the ability of the VMH to increase the blood glucose concentration (8). Electromagnetic manipulation also showed that activation of the transient receptor potential vanilloid 1 (TRPV1) ion channel in glucokinase (GK)-expressing neurons of the VMH elicited a hyperglycemic response (9), whereas optogenetic stimulation of SF1 neurons via channelrhodopsin 2 (ChR2) induced hyperglycemia and enhanced the counterregulatory response to glucopenia (10).

In contrast to such elicitation of a hyperglycemic response, the VMH has been found to increase glucose utilization and insulin sensitivity in some peripheral tissues. Electrical stimulation of the VMH increases glucose utilization in interscapular BAT, heart, and skeletal muscle, but not in white adipose tissue (WAT), as well as induces hepatic glucose production (11). Leptin, which increases the activity of a subset of SF1 neurons in the VMH (12-14), also promotes both glucose uptake in peripheral tissues including red-type skeletal muscle as well as endogenous glucose production and thereby maintains blood glucose levels (15-17). Under hyperinsulinemic-euglycemic clamp conditions, leptin acting via the VMH enhanced both insulin-induced glucose utilization in some peripheral tissues including red-type skeletal muscle and suppression of hepatic glucose production (17). The VMH contains a heterogeneous population of neurons. A subset of VMH neurons expresses the long form of the leptin receptor (18), and most of these neurons also express SF1 (12, 19). Whereas SF1 neurons in the VMH are required for maintenance of normal glucose and energy metabolism (20-22) and mediate the anorexic and metabolic effects of leptin (12, 19, 23, 24), specific activation of leptin receptor-expressing neurons in the VMH by optogenetic stimulation of ChR2 did not induce hyperglycemia (10).

DREADD (designer receptors exclusively activated by designer drugs) technology allows spatial and temporal control of the activity of specific neurons. The hM3Dq designer receptor activates signaling by the G protein Gq, and its expression and activation in SF1 neurons of the VMH may therefore have effects on glucose and energy metabolism distinct from those of

optogenetic stimulation via ChR2 (25). In the present study, we activated SF1 neurons in the VMH of mice via hM3Dq. Such activation increased whole-body glucose utilization, glucose uptake in some peripheral tissues -including red-type skeletal muscle, heart, and BAT- as well as endogenous glucose production and glycogen phosphorylase *a* activity in the liver, thereby maintaining blood glucose levels. During a hyperinsulinemic-euglycemic clamp, activation of SF1 neurons by hM3Dq; increased insulin-induced glucose uptake in the same peripheral tissues and tended to enhance insulin-induced suppression of endogenous glucose production. In addition, activation of SF1 neurons by DREADD technology suppressed food intake and increased energy expenditure.

RESEARCH DESIGN AND METHODS

Animals

SF1-Cre recombinase (SF1-Cre) transgenic mice [Stock Tg (Nr5a1-cre) 7Lowl/J] were obtained from The Jackson Laboratory (Bar Harbor, ME) (12). Heterozygous transgenic mice were crossed with FVB/N Jcl mice (Clea, Tokyo, Japan), and the genotype of the resulting offspring was determined by PCR analysis (see Supplemental Table for primer sequences). Mice were housed individually in plastic cages at 24° ± 2°C with lights on from 0600 to 1800 hours, and they were given free access to laboratory chow (CE-2 diet, Clea) and water. All experiments were performed at the same room temperature and under the same light-dark cycle. Only male SF1-Cre or wild-type (WT) mice (12 to 16 weeks of age) were used in the present study. All animal experiments were performed in accordance with institutional guidelines for the care and handling of experimental animals, and they were approved by the Institutional Animal Care and Use Committee (IACUC) of the National Institutes of Natural Sciences (Okazaki, Japan).

Surgical procedures

Stainless steel cannulas were implanted bilaterally into the VMH of WT or SF1-Cre mice at 12 to 14 weeks of age as described previously (17). The stereotaxic coordinates for the position of the VMH (AP, 1.32 mm caudal to the bregma; H, 5.72 mm below the surface of the skull; L, 0.3 mm lateral to the bregma on each side) were obtained from the Mouse Brain Atlas (26). For measurement of 2-deoxyglucose (2DG) uptake and hyperinsulinemic-euglycemic clamp

analysis, surgery for implantation of self-made polyethylene-silicone catheters into the right jugular vein and carotid artery was performed 3 days before experiments (17).

Preparation and injection of an AAV vector and administration of CNO

Two weeks after cannula implantation, 500 nl (1.9×10^{10} copies μl^{-1}) of an adeno-associated virus (AAV, serotype 2) encoding AAV-hSyn-DIO-hM3Dq-mCherry-WPRE (AAV-hM3Dq) (25, 27) were injected into each side of the VMH of SF1-Cre mice at a rate of 50 nl/min with the use of a pump (to yield SF1-Cre:AAV-hM3Dq mice). The DREADD plasmid is based on the FLEX Switch system, which relies on two pairs of heterotypic, antiparallel loxP-type recombination sites to achieve Cre-mediated transgene inversion and expression of an hM3Dq-mCherry fusion protein under the control of the mouse synapsin 1 gene promoter. It was obtained from B. L. Roth (25, 27) and was expanded and packaged with the use of an AAV helper-free packaging system (Cell Biolabs, San Diego, CA). Mice were used for experiments 2 weeks after infection. With the exception of hyperinsulinemic-euglycemic clamp experiments, clozapine-*N*-oxide (CNO) (3 mg kg^{-1}) (Enzo Life Sciences, Farmingdale, NY) was injected intraperitoneally into SF1-Cre:AAV-hM3Dq mice to activate the DREADD receptor hM3Dq, with PBS (saline) being injected into the same mice on a different day as a control. Half of mice were injected first with saline and others with CNO, with there being no difference in the effects of CNO between mice injected first with CNO or with saline. For hyperinsulinemic-euglycemic clamp analysis, CNO (3 mg kg^{-1}) or saline was injected into SF1-Cre:AAV-hM3Dq mice through a jugular vein catheter. Preliminary experiments showed that injection of a low dose (0.3 mg kg^{-1}) of CNO had no effect on food intake or whole-body glucose metabolism in SF1-Cre:AAV-hM3Dq mice (data not shown). Furthermore, the effects of bilateral injection of CNO (30 μM; 1.5 pmol in 50 nl of physiological saline) into the VMH on food intake and in an insulin tolerance test (ITT) were similar to those of intraperitoneal injection. We therefore adopted intraperitoneal or intravenous injection of CNO (3 mg kg^{-1}). To examine whether hM3Dq is expressed in SF1 neurons in a Cre recombinase-dependent manner, we also injected AAV-hM3Dq into the VMH of WT mice (WT:AAV-hM3Dq mice).

Immunofluorescent analysis of hM3Dq-mCherry and cfos expression

To validate the activation of SF1 neurons by hM3Dq *in vivo*, AAV-hM3Dq was unilaterally infected into the VMH of SF1-Cre mice. The contralateral side of the VMH was used as a control in the same mice. Mice were injected intraperitoneally with CNO 2 weeks after the infection, and 60 min later, mice were anesthetized with ketamine and xylazine and perfused transcardially with 4% paraformaldehyde in 0.1 mol/L phosphate buffer. Brain tissue was removed, fixed again, and embedded in OCT compound (Sakura Finetechnical, Tokyo, Japan). Serial cryosections (thickness of 7 μm) were exposed to 10% normal horse serum (Santa Cruz Biotechnology) for 1 h at room temperature, and incubated first overnight at 4ºC with rabbit polyclonal antibodies for cfos (1:200 dilution, Santa Cruz Biotechnology) and then for 90 min at room temperature with Alexa 488–labelled donkey antibodies for rabbit immunoglobulin G (1:400, Life Technologies). To validate endogenous fluorescence of mCherry in SF1-Cre:AAV-hM3Dq and WT:AAV-hM3Dq mice, those mice were also deeply anesthetized and perfused transcardially with 4% paraformaldehyde in 0.1 M phosphate buffer. Fluorescence of mCherry and Alexa 488 was detected by a fluorescence microscope (AX-70, Olympus, Tokyo, Japan).

Basal blood glucose concentration and intraperitoneal GTT and ITT analyses

To examine the effect of activation of SF1 neurons in the VMH on basal blood glucose levels, we deprived SF1-Cre:AAV-hM3Dq mice of food for 3 h and then injected them intraperitoneally with saline or CNO at time $t = 0$. Blood was collected from the tail vein at the indicated times for measurement of blood glucose concentration with the use of a One Touch Ultra glucometer (Life Scan Japan, Johnson & Johnson, Tokyo, Japan). For a glucose tolerance test (GTT), SF1-Cre:AAV-hM3Dq mice were deprived of food overnight for 16 h and then injected intraperitoneally first with saline or CNO at $t = -180$ min and then with glucose (2 g kg^{-1}) at $t = 0$. Blood glucose and plasma insulin concentrations were measured with the use of a One Touch Ultra glucometer and an insulin enzyme-linked immunosorbent assay (ELISA) kit (Shibayagi, Gunma, Japan). For an ITT, SF1-Cre:AAV-hM3Dq mice were deprived of food immediately before intraperitoneal injection with saline or CNO at $t = -180$ min. They were injected intraperitoneally with insulin (1 U kg^{-1}) (Sigma-Aldrich Japan, Tokyo) at $t = 0$, and blood glucose concentration was measured at the indicated times.

Hyperinsulinemic-euglycemic clamp and 2DG uptake

A hyperinsulinemic-euglycemic clamp was imposed and 2DG uptake was measured in conscious and free-moving mice as previously described (17). Jugular vein and carotid artery catheters were connected to an infusion pump and a saline-filled syringe, respectively, at 4 h before the start of the experiment, after which time only water was available. CNO (3 mg kg^{-1}) or saline was injected through the jugular vein catheter at t = -180 min in SF1-Cre:AAV-hM3Dq mice. A priming dose (5 μCi) of [3-^{3}H]glucose (American Radiolabeled Chemicals, St. Louis, MO) was also administered via the jugular vein catheter at t = -120 min and was followed by infusion of the tracer at a rate of 0.05 μCi min^{-1} until the end of the experiment. Beginning at t = 0, corresponding to the steady state condition, bovine insulin (Sigma-Aldrich Japan) was infused continuously (bolus of 16 mU kg^{-1} followed by a rate of 2.5 mU kg^{-1} min^{-1}) through the jugular vein catheter. Blood was collected from the carotid artery catheter, and blood glucose was monitored with the use of a One Touch Ultra glucometer (Life Scan Japan, Johnson & Johnson). Glucose (30%, w/v) was infused at a variable rate via the jugular vein catheter in order to maintain the blood glucose concentration at 100 mg dl^{-1}. Withdrawn erythrocytes were suspended in sterile 0.9% saline and returned to each animal.

For assessment of 2DG uptake during the basal period, mice were infused with 2-[^{14}C]DG (5 μCi) (American Radiolabeled Chemicals) through the jugular vein catheter at t = -45 min. At t = -180, -45, -40, -30, -20, -10, and 0 min, arterial blood samples (50 μl) were collected for assessment of the rate of blood glucose appearance (Ra) and disappearance (Rd), which reflect endogenous glucose production and whole-body glucose utilization, respectively, as well as of 2DG uptake. For measurement of 2DG uptake during the clamp period, another group of mice was infused with 2-[^{14}C]DG (5 μCi) at t = 60 min, and blood samples (50 μl) were collected at t = -180, -5, 5, 10, 20, 30, 40, 50, 60, 65, 75, 85, 95, and 105 min. Rd is equal to Ra plus the glucose infusion rate (GIR) during the clamp period, whereas Rd is equal to Ra during the basal period. Rd and Ra were determined during the basal (t = -45 to 0 min) and clamp (t = 60 to 105 min) periods as described previously (17). Immediately after collection of the final blood sample (t = 0 or 105 min), soleus muscle, red (Gastro Red) and white (Gastro White) portions of the gastrocnemius, heart, interscapular BAT, spleen, inguinal WAT (iWAT), epididymal WAT (eWAT), liver, and brain (cerebral cortex) were removed and frozen in liquid nitrogen. Gastro Red was dissected from the inner surface of the muscle attached to the soleus, whereas Gastro White was dissected from the outer surface of the muscle. The plasma concentration of insulin

was measured at t = -5 and 105 min with the use of an ELISA kit (Shibayagi). Glycogen phosphorylase *a* activity in the liver was measured as described previously (17). We also determined GIR, Ra, and Rd in WT mice injected intraperitoneally with saline as well as in CNO-injected SF1-Cre mice (without infection).

Food intake

For measurement of food intake during refeeding after fasting, SF1-Cre:AAV-hM3Dq and SF1-Cre (without infection) mice were deprived of food overnight from 1700 to 0900 hours, saline or CNO was injected intraperitoneally at 0830 hours, and consumption of lab chow (CE-2, Clea) was determined during refeeding from 0900 to 1200 hours. For measurement of food intake at the start of the dark period, saline or CNO was injected 30 min before the dark period (1730 hours) into SF1-Cre:AAV-hM3Dq and SF1-Cre (without infection) mice fed ad libitum, and consumption of lab chow (CE-2, Clea) was measured over 3, 12, and 24 h after the start of the dark period.

Energy expenditure, locomotor activity, and RQ

Energy expenditure and respiratory quotient (RQ) were measured by indirect calorimetry. Gas analysis was performed with a CO_2 and O_2 mass spectrometric analyzer (Arco-2000; Arco System, Chiba, Japan). Locomotor activity was measured with the use of a force plate system (Actracer-2000, Arco System) that was placed below the cage and which detects low-intensity activities (28). Mice were acclimatized to the analytic cage for 3 days before experiments. On the day of the experiment, SF1-Cre:AAV-hM3Dq mice were deprived of food at 0800 hours (t = -1 h) and were injected with saline or CNO at 0900 hours (t = 0). The volumes of O_2 consumed ($V\!O_2$) and CO_2 produced ($V\!CO_2$) as well as locomotor activity were measured every minute from 2100 hours on the day before the experiment to 0900 hours on the day after the start of the experiment (total of 36 h). The data were averaged for each consecutive 1-h period or over 5 h. Energy expenditure and the amount of carbohydrate or fat oxidized were calculated from $V\!O_2$ and $V\!CO_2$ as described previously (29) according to the following equations: Energy expenditure (cal min^{-1}) = (3.816 × $V\!O_2$) + (1.231 × $V\!CO_2$); carbohydrate oxidation (cal min^{-1}) = [(4.51 × $V\!CO_2$) - (3.18 × $V\!O_2$)] × 4.1; fat oxidation (cal min^{-1}) = [1.67 × ($V\!O_2$ - $V\!CO_2$)] × 9.3.

RNA extraction and RT-PCR analysis

Total RNA was isolated from tissue and subjected to reverse transcription (RT) as described previously (17). The resulting cDNA was subjected either to PCR analysis or to quantitative PCR (qPCR) analysis with SYBR Green PCR Mix (Takara Bio, Shiga, Japan) in an ABI 7500 real-time PCR system (Thermo Fisher Scientific, Yokohama, Japan). Data were normalized by the amount of 36B4 mRNA. The sequences of PCR primers are shown in the Supplemental Table.

Immunoblot analysis

The extent of Akt phosphorylation was examined in soleus muscle and liver of SF1-Cre:AAV-hM3Dq mice injected with CNO or saline and subjected to a hyperinsulinemic-euglycemic clamp. It was also examined in soleus and liver of SF1-Cre:AAV-hM3Dq mice fed ad libitum and injected intraperitoneally first with saline or CNO at time t = -180 min and then with saline or insulin (1 U kg^{-1}) at t = 0, with the animals being sacrificed at t = 30 min by intraperitoneal injection of an overdose (70 mg kg^{-1}) of pentobarbital sodium. Tissue samples were prepared as described previously (17) and were subjected to immunoblot analysis with antibodies specific for phosphorylated or total forms of Akt (Cell Signaling Technology Japan, Tokyo), horseradish peroxidase-conjugated secondary antibodies (Santa Cruz Biotechnology, Dallas, TX), and enhanced chemiluminescence reagents (GE Healthcare, Tokyo, Japan).

Electrophysiology

The brain was removed from 3- to 4-month-old SF1-Cre:AAV-hM3Dq or WT mice under deep anaesthesia with isoflurane, and coronal slices of the hypothalamus (thickness, 300 μm) were prepared and transferred to artificial cerebrospinal fluid (ACSF: 126 mM NaCl, 3 mM KCl, 1.3 mM $MgSO_4$, 2.4 mM $CaCl_2$, 1.2 mM NaH_2PO_4, 26 mM $NaHCO_3$, 10 mM glucose) at 33ºC, as described previously (30). To reduce spontaneous firing of hypothalamic neurons during recording, we lowered the glucose concentration in ACSF to 5 mM. SF1 neurons in the VMH labelled with mCherry were targeted by patch pipettes with the use of a microscope (BX51, Olympus) under fluorescent and infrared differential interference contrast optics. The patch pipettes (4 to 6 MΩ) were filled with a solution containing 130 mM potassium gluconate, 8 mM KCl, 1 mM $MgCl_2$, 0.6 mM EGTA, 10 mM HEPES, 3 mM ATP (Mg^{2+} salt), 0.5 mM GTP

(disodium salt), and 10 mM sodium phosphocreatine (adjusted to pH 7.3 with KOH). Membrane potentials were recorded in the current-clamp mode at a sampling rate of 10 kHz with the use of a Multiclamp 700B amplifier (Molecular Devices, Sunnyvale, CA). Tetrodotoxin (1 μM) was added as indicated to block action potentials. We selected cells with a high seal resistance (>1 GΩ) and a low series resistance (<25 MΩ) for analysis. After at least 5 min of stable recording, the recording was continued after bath application of CNO (1 μM). To explore the effect of CNO on the activity of VMH neurons without hM3Dq expression, we examined the membrane potential of VMH neurons of WT mice in the absence or presence of CNO. Data are expressed as the average firing rate or membrane potential during 3 to 1 min before and 5 to 7 min after CNO application. A neuron was considered to be activated or inhibited when the firing rate was increased or decreased by ≥20%, respectively or when the mean potential after CNO application was 2 standard deviations (SDs) above and below the potential before CNO application, respectively.

Statistical analysis

Quantitative data are presented for individual mice and means ± SD. Comparisons among multiple groups were performed with ANOVA followed by the Tukey-Kramer post hoc test, and those between two groups were performed with the paired or unpaired Student's *t* test. A *P* value of <0.05 was considered statistically significant.

RESULTS

Expression of hM3Dq-mCherry in SF1 neurons of the VMH and hM3Dq activation by CNO

Consistent with the specific expression of SF1 in the VMH of the adult mouse brain (5-7), expression of the hM3Dq-mCherry fusion protein in the medial hypothalamus was limited to the VMH -being especially pronounced in the dorsomedial region of the nucleus- in SF1-Cre:AAV-hM3Dq mice (Fig. 1*A* and *B*). In contrast, the fusion protein was not expressed in WT mice injected with the AAV-hM3Dq vector (Fig. 1*A*). CNO injection showed a larger number of cfos and hM3Dq-positive SF1-neurons in the unilateral side of the VMH expressing hM3Dq, being especially in the dorsomedial region of the VMH, compared with that in the contralateral (control) side of the VMH without hM3Dq expression (Fig. 1*C*). Saline injection did not show

any cfos and hM3Dq-postive neurons in SF1-Cre:AAV-hM3Dq mice (data not shown). These results suggested that CNO activates SF1 neurons expressing hM3Dq.

Patch-clamp recordings from fresh VMH slices prepared from SF1-Cre:AAV-hM3Dq mice revealed that bath application of the hM3Dq ligand CNO induced depolarization and increased the firing rate in most hM3Dq-mCherry-expressing SF1 neurons (Fig. 1*D* and *E*). Among 20 hM3Dq-mCherry-positive SF1 neurons examined, CNO increased the firing rate in 14 neurons, reduced it in 4 neurons, and had no effect in 2 neurons (Fig. 1*E*). The firing rate (mean ± SD) for all 20 neurons was 0.94 ± 0.23 Hz before and 2.00 ± 0.60 Hz after CNO application ($P < 0.05$). In the presence of the Na^+-channel blocker tetrodotoxin, CNO increased the membrane potential of all five hM3Dq-mCherry-expressing SF1 neurons examined from -47.7 ± 3.4 to -42.4 ± 3.5 mV ($P < 0.05$, $n = 5$) (Fig. 1*D* and *F*). All tested neurons were thus depolarized by the application of CNO. Among 13 VMH neurons in WT mice, CNO increased the membrane potential in one neuron, decreased in one neuron, and had no effect in 11 neurons (Fig. 1*G*).

Activation of SF1 neurons reduces food intake

Given that electrical stimulation of the VMH was previously found to reduce food intake in rats (31), we examined the effect of intraperitoneal injection of CNO on food intake in SF1-Cre:AAV-hM3Dq and SF1-Cre (without AAV-hM3Dq infection) mice. CNO injection in SF1-Cre:AAV-hM3Dq mice reduced food intake during refeeding for 3 h after an overnight fast, compared with the corresponding value for the same mice injected with saline (Fig. 2*A*). It also reduced food intake during the first 3 h of the dark period but not that measured over 12 or 24 h (Fig. 2*B* and *C*). CNO did not affect food intake in SF1-Cre mice (Fig. 2*A* and *B*). These results thus suggested that a single intraperitoneal injection of CNO in SF1-Cre:AAV-hM3Dq mice reduced food intake during the subsequent 3 h by acting at the hM3Dq receptor expressed in SF1 neurons of the VMH.

Activation of SF1 neurons increases energy expenditure

We next examined the effects of activation of SF1 neurons on energy expenditure, RQ, and locomotor activity. Compared with saline, CNO significantly increased hourly energy expenditure for the first 3 h after injection in SF1-Cre:AAV-hM3Dq mice (Fig. 3*A* and

Supplemental Fig. 1), with total energy expenditure over the first 5 h also being significantly increased (Fig. 3*B*). Injection of CNO did not affect locomotor activity (Fig. 3*C* and *D*, and Supplemental Fig. 1), however, suggesting that the increased energy expenditure was independent of such activity. CNO reduced RQ compared with that observed after saline injection (Fig. 3*E* and Supplemental Fig. 1). It also increased VO_2 without affecting VCO_2 (Fig. 3*F* and *G*, and Supplemental Fig. 1), and it increased fat oxidation without affecting carbohydrate oxidation (Fig. 3*H* and *I*, and Supplemental Fig. 1). Together, these results thus suggested that activation of SF1 neurons in the VMH by DREADD technology increased energy expenditure and fat oxidation.

Activation of SF1 neurons increases insulin sensitivity in some peripheral tissues

Activation of SF1 neurons by optogenetic stimulation with ChR2 was previously shown to induce hyperglycemia (10). We therefore examined whether activation of SF1 neurons by DREADD technology might have a similar effect. We found that CNO induced only a small, nonsignificant increase in the basal blood glucose level in SF1-Cre:AAV-hM3Dq mice (Fig. 4*A*). Performance of a GTT and ITT at 30 min after CNO injection revealed that the effects of CNO on blood glucose and plasma insulin levels varied among experiments (data not shown). We previously showed that injection of leptin or a melanocortin receptor (MCR) agonist into the VMH of mice increased insulin sensitivity in red-type skeletal muscle and liver (15-17), with these effects being apparent 3 to 6 h after the injection. We therefore examined the effects of CNO injection on GTT and ITT parameters at 3 h after the injection. Blood glucose levels during the GTT were significantly lower in mice injected with CNO than in the same animals injected with saline, whereas the plasma insulin concentration did not differ between the two treatments (Fig. 4*B* and *C*). Blood glucose levels during the ITT were also significantly lower for mice injected with CNO than in the same animals injected with saline, with the blood glucose concentration declining to ≤50 mg/dl in CNO-injected mice (Fig. 4*D*). Activation of SF1 neurons by the hM3Dq receptor thus increased glucose tolerance and insulin sensitivity in mice 3 h after CNO injection.

It was possible that the circulating levels of gluconeogenic hormones such as glucagon and glucocorticoids might have been affected by the pronounced hypoglycemia induced during the ITT in CNO-injected mice. To prevent such a hypoglycemic response after insulin

administration, we examined the effects of CNO injection in SF1-Cre:AAV-hM3Dq mice subjected to a hyperinsulinemic-euglycemic clamp beginning 3 h after the injection (Fig. 5*A*). We thus initiated insulin and glucose infusion 3 h after CNO or saline injection in SF1-Cre:AAV-hM3Dq mice (Fig. 5*A*). The blood glucose concentration had not changed at 3 h after CNO injection and was maintained during the hyperinsulinemic-euglycemic clamp at a level similar to that for the saline-injected control mice (Fig. 5*B*). However, the GIR was significantly higher after CNO injection than after saline injection (Fig. 5*C*), indicating that activation of SF1 neurons by the hM3Dq receptor increased whole-body insulin sensitivity during the clamp period.

The CNO-induced increase in GIR was associated with an increase in Rd during the clamp period (Fig. 5*D*). Rd was also increased during the basal period after CNO injection (Fig. 5*D*). Given that Ra is equal to Rd in the steady state condition during the basal period, Ra was also increased during the basal period after CNO injection (Fig. 5*E*). CNO thus increased whole-body glucose turnover during the basal period. During the clamp period, Ra was significantly reduced in both saline- and CNO-injected mice but tended to be reduced to a greater extent after CNO injection (Fig. 5*E*). The plasma insulin concentration was increased ~2-fold during the clamp period compared with the basal period, with CNO injection tending to reduce the plasma insulin level during both basal and clamp periods compared with saline. These results suggested that activation of SF1 neurons in the VMH via the hM3Dq receptor enhanced whole-body insulin sensitivity under the hyperinsulinemic-euglycemic condition. There were no significant differences in blood glucose concentration, GIR, Rd, or Ra among saline-injected WT mice, CNO-injected SF1-Cre mice (without AAV-hM3Dq infection), and saline-injected SF1-Cre:AAV-hM3Dq mice (Supplemental Fig. 2), suggesting that the effects of CNO on glucose metabolism were mediated by hM3Dq expressed in SF1 neurons of the VMH.

We next examined 2DG uptake in peripheral tissues of SF1-Cre:AAV-hM3Dq mice. CNO injection increased 2DG uptake during the basal period as well as enhanced insulin-induced glucose uptake during the clamp period in red-type skeletal muscle (soleus and Gastro Red), BAT, and heart, but not in Gastro White, spleen, eWAT, iWAT, or cerebral cortex (Fig. 6*A* and *B*).

Examination of the effect of CNO on insulin signaling in soleus muscle revealed that CNO increased the phosphorylation level of Akt, a key molecule of the insulin signaling

pathway, during the clamp period (Fig. 6*C*). Given that the insulin-induced increase in Akt phosphorylation is attenuated during insulin infusion, we examined the effect of acute insulin injection on Akt phosphorylation in soleus muscle of SF1-Cre:AAV-hM3Dq mice at 3 h after intraperitoneal injection of saline or CNO. CNO enhanced the insulin-induced phosphorylation of Akt in soleus muscle apparent 30 min after insulin injection without affecting the basal level of Akt phosphorylation (Fig. 6*D*).

To explore the mechanism by which activation of SF1 neurons by hM3Dq increases Ra during the basal period and why the effect of CNO is suppressed during the clamp period, we examined the effect of CNO injection on glycogen phosphorylase *a* activity in the liver of SF1-Cre:AAV-hM3Dq mice. CNO increased glycogen phosphorylase *a* activity in the liver during the basal period, and this effect of CNO was suppressed during the clamp period (Fig. 6*E*). These results suggested that activation of SF1 neurons in the VMH stimulates hepatic glucose production via activation of glycogen phosphorylase in the liver and thereby maintains blood glucose levels.

We also determined the effects of CNO on gluconeogenic gene expression in the liver of SF1-Cre:AAV-hM3Dq mice during the basal and clamp periods. In contrast to its effect on glycogen phosphorylase *a* activity, CNO injection reduced the amounts of glucose-6-phosphatase (G6Pase) and PEPCK mRNAs in the liver during the basal period as well as enhanced the insulin-induced down-regulation of these mRNAs (Fig. 6*F* and *G*). Activation of SF1 neurons did not affect either Akt phosphorylation during the clamp period or acute insulin-induced Akt phosphorylation in the liver (Fig. 6*H* and *I*). These results suggested that activation of SF1 neurons by DREADD technology suppressed gluconeogenic gene expression in the liver in an Akt-independent manner.

DISCUSSION

We have here shown that activation of SF1 neurons by DREADD technology with the designer receptor hM3Dq increased glucose uptake and insulin sensitivity in red-type skeletal muscle, BAT, and heart. We also found that activation of SF1 neurons by hM3Dq maintained euglycemia under basal conditions, in contrast to the hyperglycemic effect of activation either of SF1 neurons by ChR2 (10) or of GK-expressing neurons in the VMH by TRPV1 (9). Activation of SF1 neurons by hM3Dq increased glycogen phosphorylase *a* activity in the liver, whereas this

effect was suppressed during a hyperinsulinemic-euglycemic clamp. These results suggest that activation of SF1 neurons by hM3Dq increases hepatic glucose production by activation of glycogen phosphorylase *a* in this tissue and thereby maintains blood glucose levels. We also found that activation of SF1 neurons by DREADD technology down-regulated the hepatic abundance of mRNAs for gluconeogenic genes, and this effect was enhanced under the hyperinsulinemic-euglycemic condition. The activation of SF1 neurons by hM3Dq thus has two distinct effects on glucose metabolism in the liver: it increases glycogen phosphorylase *a* activity, and it inhibits gluconeogenic gene expression. Together, our observations suggest that activation of SF1 neurons by hM3Dq increases glucose uptake in peripheral tissues including red-type skeletal muscle, BAT, and heart as well as glucose production in the liver. It also promotes insulin-induced glucose uptake in these peripheral tissues as well as insulin-induced suppression of gluconeogenic gene expression in the liver. We also found that activation of SF1 neurons via DREADD technology reduced food intake and increased energy expenditure.

SF1 neurons are regulated by humoral factors such as nutrients (for example, glucose) and hormones (for example, leptin and insulin) (8, 12-14, 19, 22-24). The long form of the leptin receptor is expressed in some VMH neurons (18), and leptin increases the activity of a subset of SF1 neurons in the VMH (12-14). Leptin promotes glucose uptake and insulin sensitivity in peripheral tissues including red-type skeletal muscle, BAT, and heart via VMH neurons, maintaining blood glucose levels through increased hepatic glucose production (15-17), and it promotes insulin-induced suppression of hepatic glucose production through a distinct mechanism in the VMH (17). Our present data now suggest that activation of Gq signaling in SF1 neurons by hM3Dq mimics the effects of leptin on glucose and energy metabolism but does not trigger a hyperglycemic response. These observations suggest that a subset of SF1 neurons increases insulin sensitivity in peripheral tissues, whereas another subset of SF1 neurons induces hyperglycemia and enhances the counterregulatory response to glucopenia. A previous study also suggested that hM3Dq may regulate distinct types of neurons compared with those regulated by an optogenetic approach (25). Ligation of hM3Dq may therefore activate a subset of SF1 neurons in the VMH that includes leptin receptor-expressing neurons. We have shown that injection of glutamate into the VMH induced hyperglycemia as well as glucose uptake in some peripheral tissues including red-type skeletal muscle, heart, and BAT (11). Activation of ionotropic glutamate receptors in SF1 neurons may thus induce both a hyperglycemic response

and glucose uptake in these peripheral tissues. Similarly, activation of SF1 neurons by ChR2 may induce glucose uptake preferentially in some peripheral tissues as well as hyperglycemia. However, it is also possible that the distinct effects of optogenetic and DREADD stimulation on glucose metabolism are due to the different expression of hM3Dq and ChR2 in a specific region of the VMH. In the present study, hM3Dq was expressed at a high level in the dorsomedial region of the VMH. Most leptin-activated SF1 neurons are located within the dorsomedial subdivision of the VMH (14).

Activation of SF1 neurons in the VMH increased phosphorylation of Akt in soleus muscle during the hyperinsulinemic-euglycemic clamp as well as enhanced that induced by acute injection of insulin. We previously showed that activation of VMH neurons by orexin, acting via muscle sympathetic nerves and β_2-adrenergic receptors, stimulates glucose uptake and insulin sensitivity in red-type skeletal muscle by increasing insulin delivery from blood vessels (32). Activation of SF1 neurons by DREADD technology may thus increase insulin sensitivity in red-type skeletal muscle also by enhancing insulin delivery to muscle cells. In contrast, we have shown that electrical stimulation of the VMH promotes glucose transport in heart muscle and BAT by influencing different aspects of insulin action (33). Similarly, CNO did not affect Akt phosphorylation in soleus muscle of mice without insulin infusion. Activation of SF1 neurons in the VMH may therefore increase glucose uptake in red-type skeletal muscle, heart, and BAT in both insulin-independent and -dependent manners.

Activation of SF1 neurons by DREADD technology increased glycogen phosphorylase *a* activity in the liver under basal conditions, whereas it suppressed hepatic expression of the gluconeogenic genes for G6Pase and PEPCK. The extent of Akt phosphorylation in the liver was not affected by injection of CNO with or without insulin infusion. These results suggest that activation of SF1 neurons by hM3Dq regulates hepatic glycogenolysis and gluconeogesis in an Akt-independent manner. Intracerebroventricular injection of leptin was also previously shown to regulate hepatic glycogenolysis and gluconeogenesis in a reciprocal manner (34). Further study is warranted to explore the mechanisms by which activation of SF1 neurons by hM3Dq regulates glucose metabolism in the liver.

Activation of SF1 neurons by hM3Dq suppressed food intake not only at the start of the dark period but also after an overnight fast, suggesting that activation of these neurons in the VMH via this receptor promotes satiety. A locus in the VMH -especially in the ventrolateral

region of the nucleus- has been shown to promote aggressive behavior (35), and the VMH neurons responsible for this effect are marked by expression of estrogen receptor 1 (Esr1) (36). However, we did not detect any aggression-like behavior after injection of CNO in SF1-Cre:AAV-hM3Dq mice (data not shown). In the present study, hM3Dq was expressed at a high level in the dorsomedial region of the VMH, while Esr1 is expressed in the ventrolateral region of the VMH (36). Thus, CNO did possibly not activate Esr1 expressing neurons in the ventrolateral region of the VMH. We also found that activation of SF1 neurons by hM3Dq increased energy expenditure without altering locomotor activity, with this effect being due to increased fat oxidation. These results are consistent with our previous data showing that leptin stimulates fatty acid oxidation in red-type skeletal muscle via activation of muscle AMP-activated protein kinase (AMPK) (37).

The VMH contains glucose-excitatory (GE) and glucose-inhibitory (GI) neurons (13, 14, 38). Activation of GE neurons among SF1 neurons in the VMH was recently shown to regulate insulin sensitivity in skeletal muscle and the liver via uncoupling protein 2 (UCP2) and mitochondrial fission (39). Among GE neurons in the VMH, the number of cells excited by leptin is almost twice that of those inhibited by leptin (13). Further studies are necessary to explore the effects of hM3Dq activation on GE, GI, and leptin receptor-expressing neurons in the VMH. Collectively, our results show that DREADD technology provides an important tool for investigations of the role of the central nervous system in the control of insulin sensitivity and glucose metabolism in peripheral tissues.

Acknowledgments. The authors thank Pavel Osten (Cold Spring Harbor Laboratory, Cold Spring Harbor, NY) and Bryan L. Roth [Department of Pharmacology and National Institute of Mental Health Psychoactive Drug Screening Program (NIMH PDSP), University of North Carolina School of Medicine, Chapel Hill, NC] for viral vectors, Megumi Hayashi (Division of Endocrinology and Metabolism, National Institute for Physiological Sciences) for help with manuscript preparation, Rie Kageyama (Section of Viral Vector Development, Center for Genetic Analysis of Behavior, National Institute for Physiological Sciences) for virus preparation, the Functional Genomics Facility at the National Institute for Basic Biology (NIBB) for DNA sequencing, and the Center for Radioisotope Facilities at NIBB for assistance with radioisotope experiments.

Funding. This study was supported by a Grant-in-Aid for Scientific Research (B) (24390058 to Y.M.), a Grant-in-Aid for Exploratory Research (15K15352 to Y.M.), and a Grant-in-Aid for Scientific Research (C) (15K09405 to S.O.) from the Japan Society for the Promotion of Science; a Grant-in-Aid for Scientific Research on Innovative Areas (22126005 to Y.M.) from the Ministry of Education, Culture, Sports, Science, and Technology of Japan; and by the Core Research for Evolutional Science and Technology Program (CREST) of the Japan Science and Technology Agency and the Japan Agency for Medical Research and Development (to Y.M.).

Duality of Interest. No potential conflicts of interest relevant to this article were reported.

Author Contributions. E.A.C. and Y.M. designed the experiments, analyzed the data, and wrote the manuscript. E.A.C. performed GTT and hyperinsulinemic-euglycemic clamp analyses. E.A.C. and S.O. performed the ITT and histological experiments. E.A.C. and K.T. performed energy expenditure experiments. E.A.C., S.O., T.S., and K.K. prepared and evaluated viral vectors. E.A.C., K.S., S.Y., and C.-C.W. performed biochemical experiments. A.I. and Y.Y. performed electrophysiological experiments. N.W, T.H. and S.S. supervised the histological experiments. Y.O. supervised the project. Y.M. is the guarantor of this work and, as such, had full access to all the data in the study and takes responsibility for the integrity of the data and the accuracy of the data analysis.

REFERENCES

1. Swanson LW. The hypothalamus. In *Handbook of Chemical Neuroanatomy*, vol 5. *Integrated Systems of the CNS*, part 1. Björklund A, Hökfelt T, Swanson LW, Eds. Amsterdam, Elsevier, 1987, p. 1-124
2. Grayson BE, Seeley RJ, Sandoval DA. Wired on sugar: the role of the CNS in the regulation of glucose homeostasis. Nat Rev Neurosci 2013;14:24-37
3. Morton GJ, Schwartz MW. Leptin and the central nervous system control of glucose metabolism. Physiol Rev 2011;91:389-411
4. Shimazu T, Fukuda A, Ban T. Reciprocal influences of the ventromedial and lateral hypothalamic nuclei on blood glucose level and liver glycogen content. Nature 1966;210:1178-1179
5. Majdic G, Young M, Gomez-Sanchez E, Anderson P, Szczepaniak LS, Dobbins RL, McGarry JD, Parker KL. Knockout mice lacking steroidogenic factor 1 are a novel genetic model of hypothalamic obesity. Endocrinology 2002;143:607-614
6. Zhao L, Bakke M, Hanley NA, Majdic G, Stallings NR, Jeyasuria P, Parker KL. Tissue-specific knockouts of steroidogenic factor 1. Mol Cell Endocrinol 2004;215:89-94
7. Shima Y, Zubair M, Ishihara S, Shinohara Y, Oka S, Kimura S, Okamoto S, Minokoshi Y, Suita S, Morohashi K. Ventromedial hypothalamic nucleus-specific enhancer of Ad4BP/SF-1 gene. Mol Endocrinol 2005;19:2812-2823
8. Tong Q, Ye C, McCrimmon RJ, Dhillon H, Choi B, Kramer MD, Yu J, Yang Z, Christiansen LM, Lee CE, Choi CS, Zigman JM, Shulman GI, Sherwin RS, Elmquist JK, Lowell BB. Synaptic glutamate release by ventromedial hypothalamic neurons is part of the neurocircuitry that prevents hypoglycemia. Cell Metab 2007;5:383-393
9. Stanley SA, Kelly L, Latcha KN, Schmidt SF, Yu X, Nectow AR, Sauer J, Dyke JP, Dordick JS, Friedman JM. Bidirectional electromagnetic control of the hypothalamus regulates feeding and metabolism. Nature 2016;531:647-650
10. Meek TH, Nelson JT, Matsen ME, Dorfman MD, Guyenet SJ, Damian V, Allison MB, Scarlett JM, Nguyen HT, Thaler JP, Olson DP, Myers MG Jr, Schwartz MW, Morton GJ. Functional identification of a neurocircuit regulating blood glucose. Proc Natl Acad Sci USA 2016;113:E2073-E2082

11. Sudo M, Minokoshi Y, Shimazu T. Ventromedial hypothalamic stimulation enhances peripheral glucose uptake in anesthetized rats. Am J Physiol 1991;261:E298-E303
12. Dhillon H, Zigman JM, Ye C, Lee CE, McGovern RA, Tang V, Kenny CD, Christiansen LM, White RD, Edelstein EA, Coppari R, Balthasar N, Cowley MA, Chua S Jr, Elmquist JK, Lowell BB. Leptin directly activates SF1 neurons in the VMH, and this action by leptin is required for normal body-weight homeostasis. Neuron 2006;49:191-203
13. Irani BG, Le Foll C, Dunn-Meynell A, Levin BE. Effects of leptin on rat ventromedial hypothalamic neurons. Endocrinology 2008;149:5146-5154
14. Sohn JW, Oh Y, Kim KW, Lee S, Williams KW, Elmquist JK. Leptin and insulin engage specific PI3K subunits in hypothalamic SF1 neurons. Mol Metab 2016;5:669-679
15. Minokoshi Y, Haque MS, Shimazu T. Microinjection of leptin into the ventromedial hypothalamus increases glucose uptake in peripheral tissues in rats. Diabetes 1999;48:287-291
16. Toda C, Shiuchi T, Lee S, Yamato-Esaki M, Fujino Y, Suzuki A, Okamoto S, Minokoshi Y. Distinct effects of leptin and a melanocortin receptor agonist injected into medial hypothalamic nuclei on glucose uptake in peripheral tissues. Diabetes 2009;58:2757-2765
17. Toda C, Shiuchi T, Kageyama H, Okamoto S, Coutinho EA, Sato T, Okamatsu-Ogura Y, Yokota S, Takagi K, Tang L, Saito K, Shioda S, Minokoshi Y. Extracellular signal-regulated kinase in the ventromedial hypothalamus mediates leptin-induced glucose uptake in red-type skeletal muscle. Diabetes 2013;62:2295-2307
18. Elmquist JK, Bjørbæk C, Ahima RS, Flier JS, Saper CB. Distributions of leptin receptor mRNA isoforms in the rat brain. J Comp Neurol 1998;395:535-547
19. Bingham NC, Anderson KK, Reuter AL, Stallings NR, Parker KL. Selective loss of leptin receptors in the ventromedial hypothalamic nucleus results in increased adiposity and a metabolic syndrome. Endocrinology 2008;149:2138-2148
20. Zhang R, Dhillon H, Yin H, Yoshimura A, Lowell BB, Maratos-Flier E, Flier JS. Selective inactivation of Socs3 in SF1 neurons improves glucose homeostasis without affecting body weight. Endocrinology 2008;149:5654-5661
21. Xu Y, Hill JW, Fukuda M, Gautron L, Sohn JW, Kim KW, Lee CE, Choi MJ, Lauzon DA, Dhillon H, Lowell BB, Zigman JM, Zhao JJ, Elmquist JK. PI3K signaling in the

ventromedial hypothalamic nucleus is required for normal energy homeostasis. Cell Metab 2010;12:88-95

22. Klöckener T, Hess S, Belgardt BF, Paeger L, Verhagen LA, Husch A, Sohn JW, Hampel B, Dhillon H, Zigman JM, Lowell BB, Williams KW, Elmquist JK, Horvath TL, Kloppenburg P, Brüning JC. High-fat feeding promotes obesity via insulin receptor/PI3K-dependent inhibition of SF-1 VMH neurons. Nat Neurosci 2011;14:911-918
23. Kim KW, Zhao L, Donato J Jr, Kohno D, Xu Y, Elias CF, Lee C, Parker KL, Elmquist JK. Steroidogenic factor 1 directs programs regulating diet-induced thermogenesis and leptin action in the ventral medial hypothalamic nucleus. Proc Natl Acad Sci USA 2011;108:10673-10678
24. Meek TH, Matsen ME, Dorfman MD, Guyenet SJ, Damian V, Nguyen HT, Taborsky GJ Jr, Morton GJ. Leptin action in the ventromedial hypothalamic nucleus is sufficient, but not necessary, to normalize diabetic hyperglycemia. Endocrinology 2013;154:3067-3076
25. Alexander GM, Rogan SC, Abbas AI, Armbruster BN, Pei Y, Allen JA, Nonneman RJ, Hartmann J, Moy SS, Nicolelis MA, McNamara JO, Roth BL. Remote control of neuronal activity in transgenic mice expressing evolved G protein-coupled receptors. Neuron 2009;63:27-39
26. Paxinos G, Franklin K. *The Mouse Brain in Stereotaxic Coordinates*. 3rd ed. San Diego, CA, Academic Press, 2007
27. Krashes MJ, Koda S, Ye C, Rogan SC, Adams AC, Cusher DS, Maratos-Flier E, Roth BL, Lowell BB. Rapid, reversible activation of AgRP neurons drives feeding behavior in mice. J Clin Invest 2011;121:1424-1428
28. Virtue S, Even P, Vidal-Puig A. Below thermoneutrality, changes in activity do not drive changes in total daily energy expenditure between groups of mice. Cell Metab 2012;16:665-671
29. Ishihara K, Oyaizu S, Onuki K, Lim K, Fushiki T. Chronic (-)-hydroxycitrate administration spares carbohydrate utilization and promotes lipid oxidation during exercise in mice. J Nutr 2000;130:2990-2995
30. Ishikawa AW, Komatsu Y, Yoshimura Y. Experience-dependent emergence of fine-scale networks in visual cortex. J Neurosci 2014;34:12576-12586

31. Beltt BM, Keesey RE. Hypothalamic map of stimulation current thresholds for inhibition of feeding in rats. Am J Physiol 1975;229:1124-1133
32. Shiuchi T, Haque MS, Okamoto S, Inoue T, Kageyama H, Lee S, Toda C, Suzuki A, Bachman ES, Kim YB, Sakurai T, Yanagisawa M, Shioda S, Imoto K, Minokoshi Y. Hypothalamic orexin stimulates feeding-associated glucose utilization in skeletal muscle via sympathetic nervous system. Cell Metab 2009;10:466-480
33. Takahashi A, Sudo M, Minokoshi Y, Shimazu T. Effects of ventromedial hypothalamic stimulation on glucose transport system in rat tissues. Am J Physiol 1992;263:R1228-R1234
34. Liu L, Karkanias GB, Morales JC, Hawkins M, Barzilai N, Wang J, Rossetti L. Intracerebroventricular leptin regulates hepatic but not peripheral glucose fluxes. J Biol Chem 1998;273:31160-31167
35. Lin D, Boyle MP, Dollar P, Lee H, Lein ES, Perona P, Anderson DJ. Functional identification of an aggression locus in the mouse hypothalamus. Nature 2011;470:221-226
36. Lee H, Kim DW, Remedios R, Anthony TE, Chang A, Madisen L, Zeng H, Anderson DJ. Scalable control of mounting and attack by $Esr1^{+}$ neurons in the ventromedial hypothalamus. Nature 2014;509:627-632
37. Minokoshi Y, Kim YB, Peroni OD, Fryer LG, Müller C, Carling D, Kahn BB. Leptin stimulates fatty-acid oxidation by activating AMP-activated protein kinase. Nature 2002;415:339-343
38. Kang L, Dunn-Meynell AA, Routh VH, Gaspers LD, Nagata Y, Nishimura T, Eiki J, Zhang BB, Levin BE. Glucokinase is a critical regulator of ventromedial hypothalamic neuronal glucosensing. Diabetes 2006;55:412-420
39. Toda C, Kim JD, Impellizzeri D, Cuzzocrea S, Liu ZW, Diano S. UCP2 regulates mitochondrial fission and ventromedial nucleus control of glucose responsiveness. Cell 2016;164:872-883

FIGURE LEGENDS

Figure 1. Expression of hM3Dq-mCherry in SF1 neurons of the VMH and electrophysiological validation of the DREADD system. *A*: Expression of hM3Dq-mCherry in SF1 neurons of the VMH of an SF1-Cre:AAV-hM3Dq mouse (coronal and sagittal sections) but not in those of a WT:AAV-hM3Dq mouse (coronal section) as revealed by the intrinsic fluorescence of mCherry (left images). Photomicrographs of the same hypothalamic sections are also shown (right images). Scale bars, 100 μm. *B*: RT-PCR analysis of Cre recombinase, SF1, and glyceraldehyde-3-phosphate dehydrogenase (G3PDH, internal control) mRNAs in the arcuate nucleus (ARH), VMH, and dorsomedial (DMH) and paraventricular (PVH) hypothalamus of SF1-Cre mice. *C*: cfos expression in the VMH of SF1-Cre mice. AAV-hM3Dq were infected into the unilateral side of the VMH. Yellow and orange arrow heads indicate a cfos-positive neuron with and without expression of hM3Dq, respectively. *D*: Representative recordings of action potentials (upper trace) and membrane potential (lower trace) from an hM3Dq-mCherry-expressing SF1 neuron in a freshly prepared tissue slice. The duration of bath application of CNO (1 μM) is indicated by the bars. The membrane potential was recorded in the presence of tetrodotoxin (TTX). *E*: Firing rate (mean ± SD and individual neurons) of hM3Dq-mCherry-expressing SF1 neurons ($n = 20$) before and after application of CNO (left panel) as well as the relative change in firing rate of individual neurons induced by CNO (right panel). Red, gray, and blue indicate neurons that show an increase (≥20%), no change (<20%), or decrease (≥20%) in firing rate, respectively. *F*: Membrane potential of hM3Dq-mCherry-expressing SF1 neurons ($n = 5$) in the presence of tetrodotoxin before and after application of CNO. Data are for individual neurons and mean ± SD (left) and delta increase (right) of the membrane potential. *G*: Membrane potential of VMH neurons of wild type mice before and after application of CNO ($n = 13$ neurons). Data are for individual neurons and mean ± SD (left) and delta change (left) of the membrane potential. Block and white circles indicate neurons that show an increase or decrease (≥2 SDs) and no change (<2 SDs) in membrane potential, respectively. $^*P < 0.05$ versus before CNO application (paired Student's *t* test).

Figure 2. Activation of SF1 neurons reduces food intake. *A*: Food intake was measured over 3 h of refeeding with lab chow after an overnight fast for 16 h in SF1-Cre mice infected ($n = 13$) or not ($n = 6$) with AAV-hM3Dq. *B*: Food intake was measured during the first 3 h of the dark

period with lab chow freely available in SF1-Cre mice infected (n = 6) or not (n = 5) with AAV-hM3Dq. *C*: Food intake was measured over 12 or 24 h after the start of the dark period with lab chow freely available in SF1-Cre:AAV-hM3Dq mice (n = 4). For all experiments, CNO or saline was injected intraperitoneally 30 min before measurement of food intake in the same mice on different days. Data are for individual mice and means ± SD. *P < 0.05 versus corresponding value for saline injection.

Figure 3. Activation of SF1 neurons increases energy expenditure and fat oxidation. SF1-Cre:AAV-hM3Dq mice were deprived of food for 1 h and then injected intraperitoneally with CNO or saline (same animals, different days) at t = 0 for measurement of energy expenditure (*A*), locomotor activity (*C*), RQ (*E*), VO_2 (*F*), VCO_2 (*G*), fat oxidation (*H*), and carbohydrate oxidation (*I*). Total energy expenditure (*B*) and locomotor activity (*D*) over 6 h were also calculated. Data are means ± SD (n = 6). Bar graphs also show the data for individual mice. *P < 0.05 versus corresponding saline value. See Supplemental Fig. 1 for measurements over 36 h.

Figure 4. Effects of activation of SF1 neurons on blood glucose level, GTT and ITT. *A*: Basal blood glucose level after intraperitoneal injection of saline or CNO at t = 0 min in the same SF1-Cre:AAV-hM3Dq mice (n = 9) on different days. The mice were deprived of food for 3 h before measurements. *B* and *C*: Blood glucose (*B*) and plasma insulin (*C*) levels during a GTT performed 3 h after intraperitoneal injection of saline or CNO in the same SF1-Cre:AAV-hM3Dq mice (n = 5) on different days. Mice were deprived of food overnight before the test, and glucose (2 g kg^{-1}) was injected intraperitoneally at t = 0. *D*: Blood glucose level during an ITT performed 3 h after intraperitoneal injection of saline or CNO in the same SF1-Cre:AAV-hM3Dq mice (n = 7) on different days. Mice were fed ad libitum until injection of saline or CNO, and insulin (1 U kg^{-1}) was injected intraperitoneally at t = 0. All data are means ± SD. *P < 0.05 versus corresponding value for saline injection.

Figure 5. Activation of SF1 neurons increases whole-body insulin sensitivity. *A*: Experimental protocol for the hyperinsulinemic-euglycemic clamp and measurement of 2DG uptake. SF1-Cre:AAV-hM3Dq mice were injected intravenously (i.v.) with saline or CNO at t = -180 min. *B*: Blood glucose concentration before and after insulin infusion for the hyperinsulinemic-

euglycemic clamp. *C*: Glucose infusion rate (GIR) during the hyperinsulinemic-euglycemic clamp (left panel) and mean GIR during the final 45 min of the clamp period (right panel). *D*: Rate of glucose disappearance (Rd) during the basal and clamp periods. *E*: Rate of glucose appearance (Ra) during the basal and clamp periods (left panel) as well as the percentage suppression of Ra induced by insulin infusion (right panel). *F*: Plasma insulin level during the basal and clamp periods. All data are means ± SD for mice injected saline (n = 7) and CNO (n = 6), with the exception of mice injected CNO in Fig. 5*F* (n = 4). Bar graphs also show the data for individual mice. *P < 0.05 versus saline injection and basal period; †P < 0.05 versus CNO injection and basal period; ‡P < 0.05 versus saline injection and clamp period.

Figure 6. Activation of SF1 neurons increases insulin sensitivity in peripheral tissues. *A* and *B*: Rates of 2DG uptake in skeletal muscle (soleus, Gastro Red, Gastro White) (*A*) as well as heart, interscapular BAT, spleen, eWAT, iWAT, and brain (cerebral cortex) (*B*) of SF1-Cre:AAV-hM3Dq mice injected with saline (n = 7) or CNO (n = 6). Data are shown for basal and clamp periods. *C*: Immunoblot analysis of the relative ratio of phosphorylated (p) to total (t) forms of Akt in soleus during the clamp period for SF1-Cre:AAV-hM3Dq mice injected with saline (n = 7) or CNO (n = 4). *D*: Representative immunoblot analysis and quantitation of the relative pAkt/tAkt ratio in soleus of SF1-Cre:AAV-hM3Dq mice at 30 min after intraperitoneal injection of insulin (1 U kg^{-1}) or saline. CNO (or saline) was injected intraperitoneally 180 min before insulin (or saline) injection. With the exception of CNO + Insulin (n = 7), n = 5 mice for each group. *E*: Glycogen phosphorylase *a* activity in the liver during basal and clamp periods for SF1-Cre:AAV-hM3Dq mice injected with saline (n = 7) or CNO (n = 5). *F* and *G*: RT-qPCR analysis of the relative amounts of G6Pase (*F*) and PEPCK (*G*) mRNAs during the basal and clamp periods for SF1-Cre:AAV-hM3Dq mice injected with saline (n = 7) or CNO (n = 4). *H*: Immunoblot analysis of the relative pAkt/tAkt ratio in the liver during the clamp period for SF1-Cre:AAV-hM3Dq mice injected with saline (n = 5) or CNO (n = 4). *I*: Representative immunoblot analysis and quantitation of the relative pAkt/tAkt ratio in the liver of SF1-Cre:AAV-hM3Dq mice at 30 min after intraperitoneal injection of insulin (1 U kg^{-1}) or saline. CNO (or saline) was injected intraperitoneally 180 min before insulin (or saline) injection. With the exception of CNO + Insulin (n = 7), n = 5 mice for each group. All quantitative data are for individual mice and means ± SD. *P < 0.05 versus saline injection and basal period or Saline +

Saline; †$P < 0.05$ versus CNO injection and basal period or CNO + Saline; ‡$P < 0.05$ versus saline injection and clamp period or Saline + Insulin.

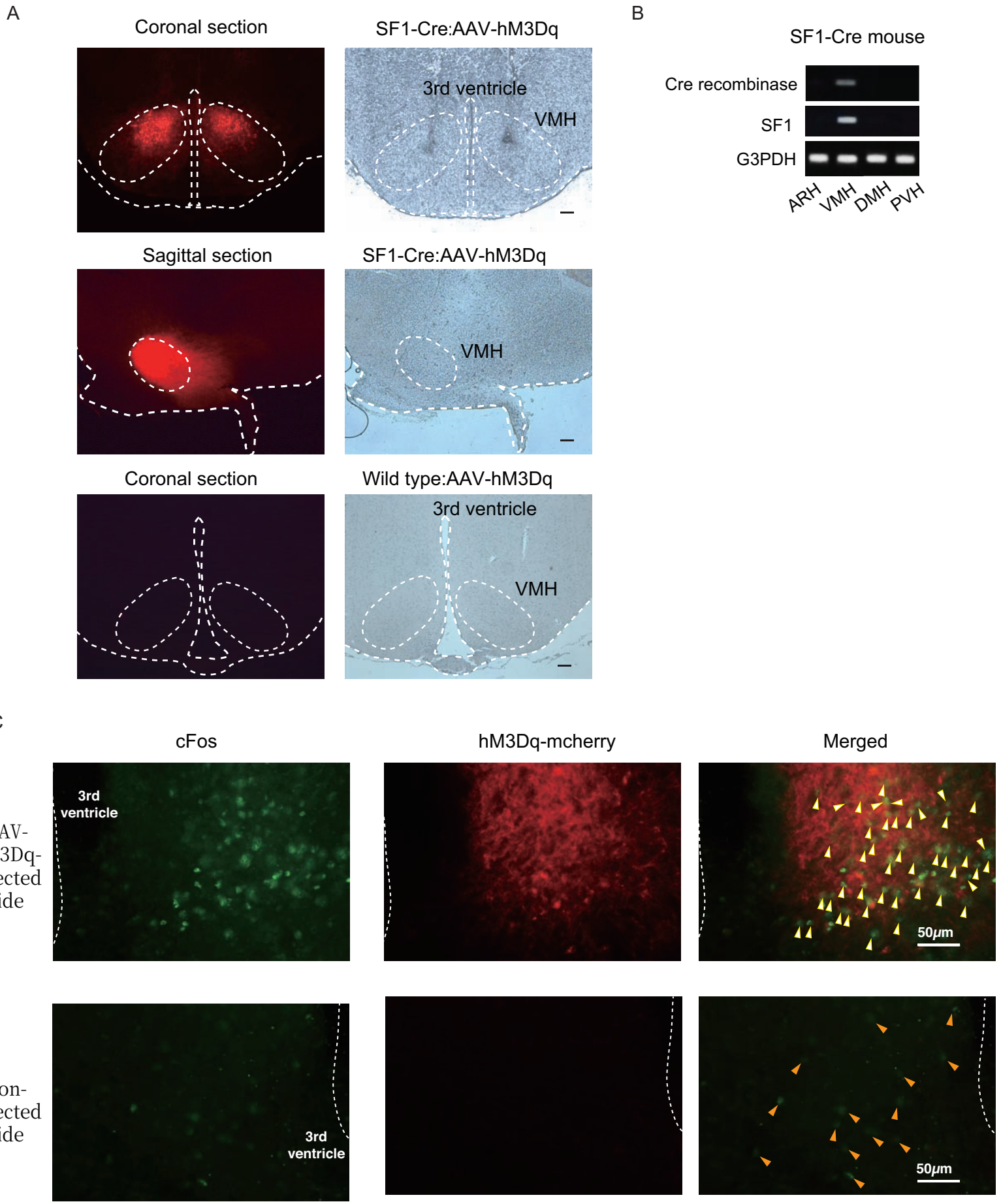

Figure 1

208x258mm (300 x 300 DPI)

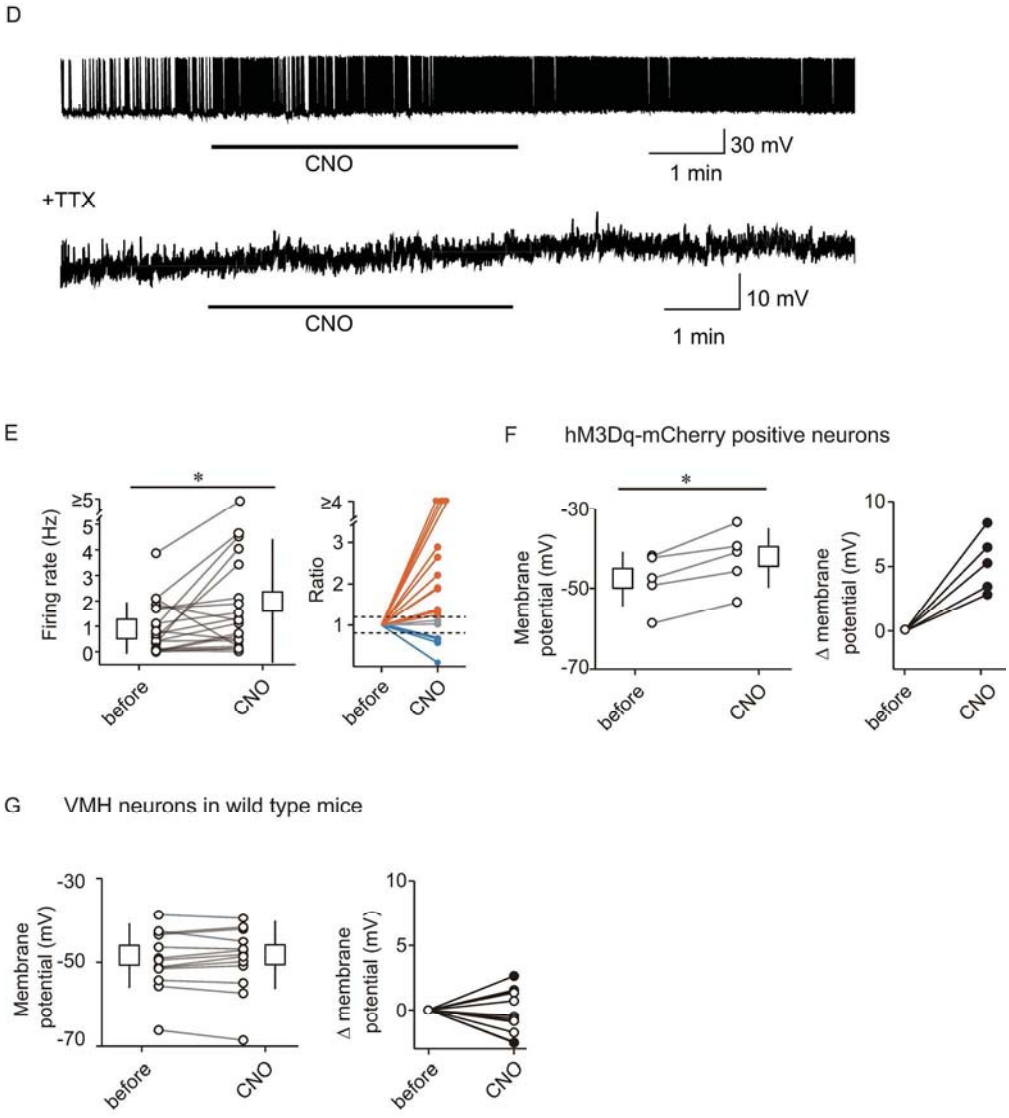

Figure 1 (continued)

198x220mm (300 x 300 DPI)

Figure 2

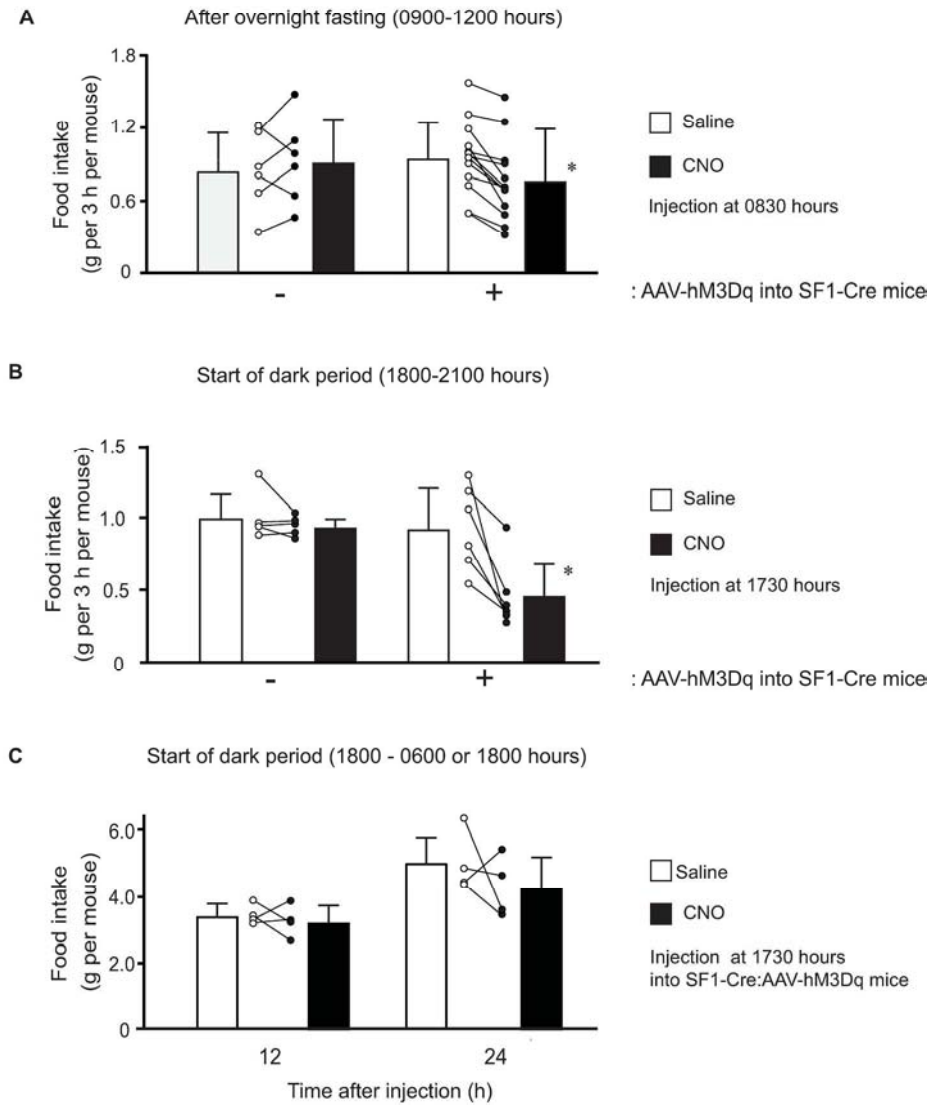

Figure 2

225x280mm (300 x 300 DPI)

Figure 3

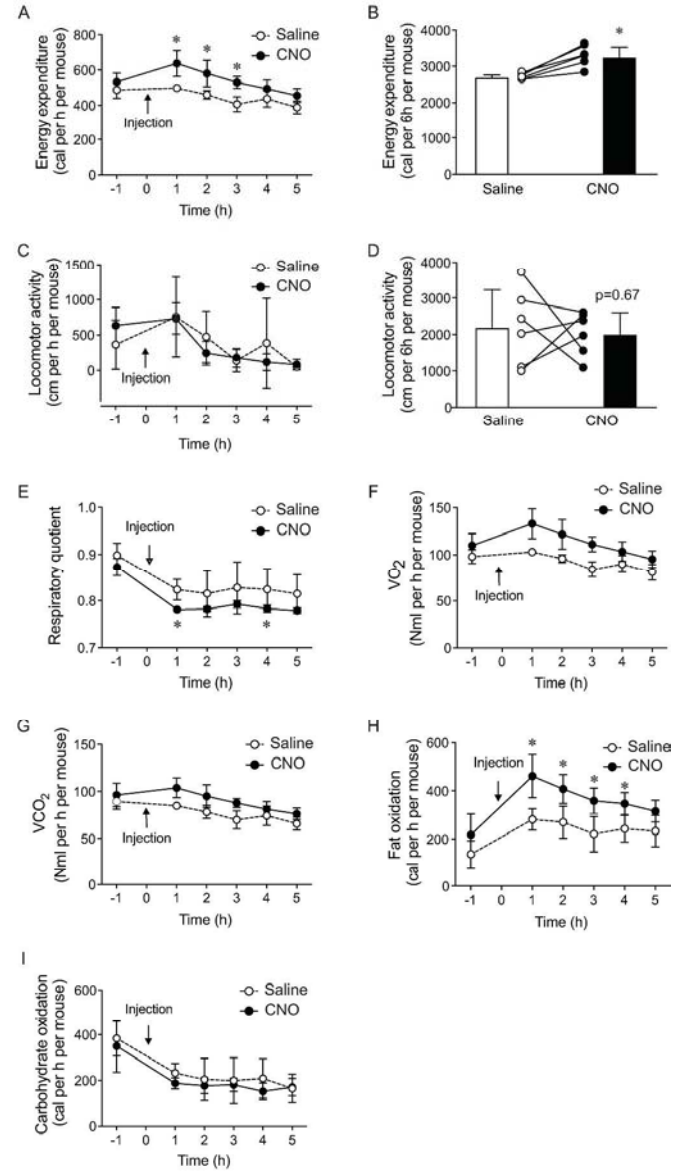

Figure 3

292x525mm (300 x 300 DPI)

Figure 4

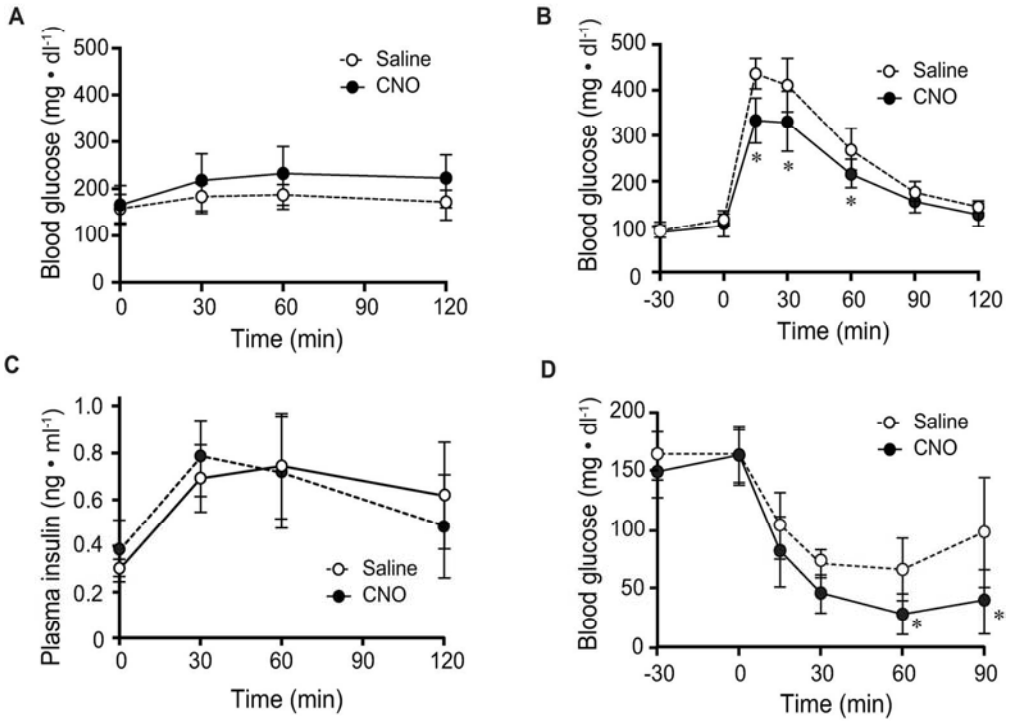

Figure 4

130x102mm (300 x 300 DPI)

Figure 5

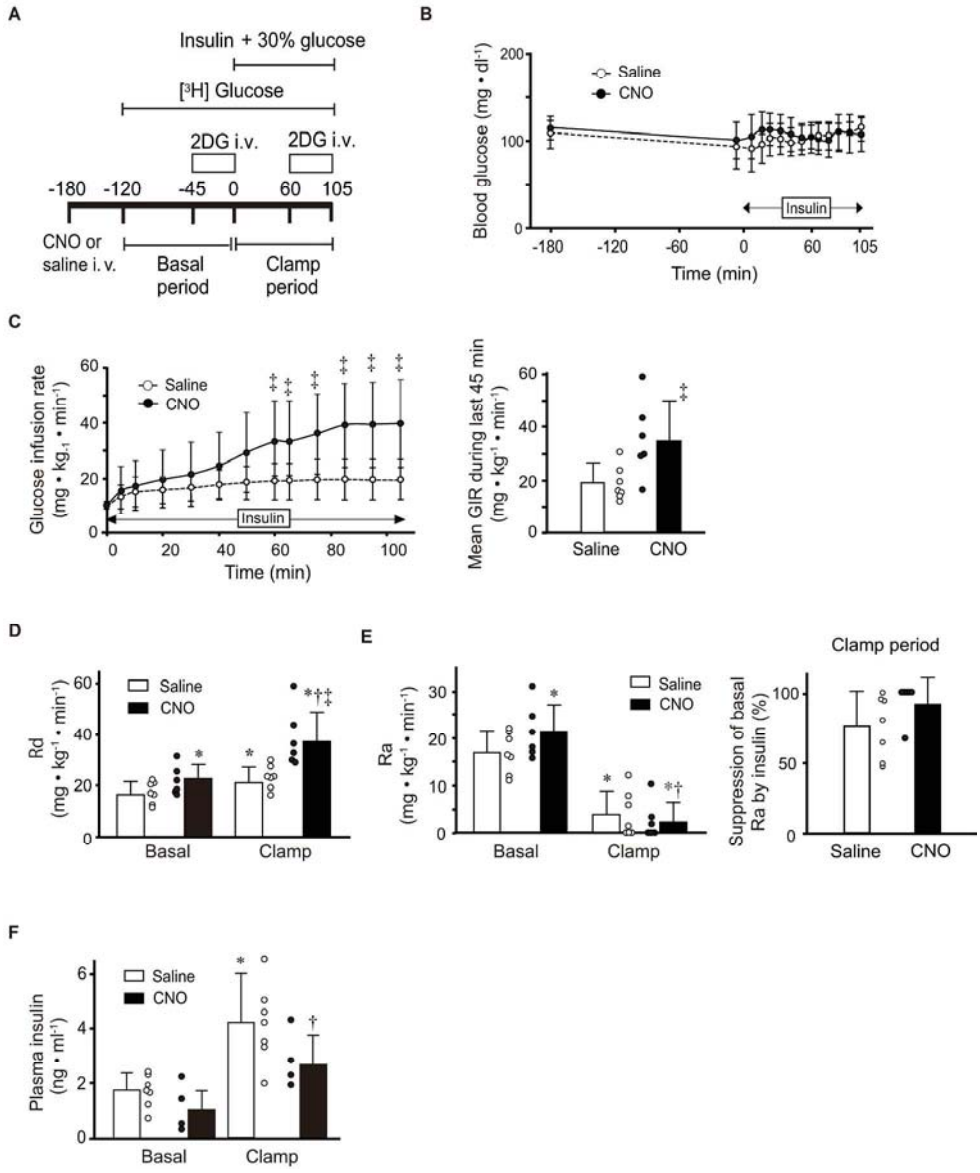

Figure 5

255x315mm (300 x 300 DPI)

Figure 6

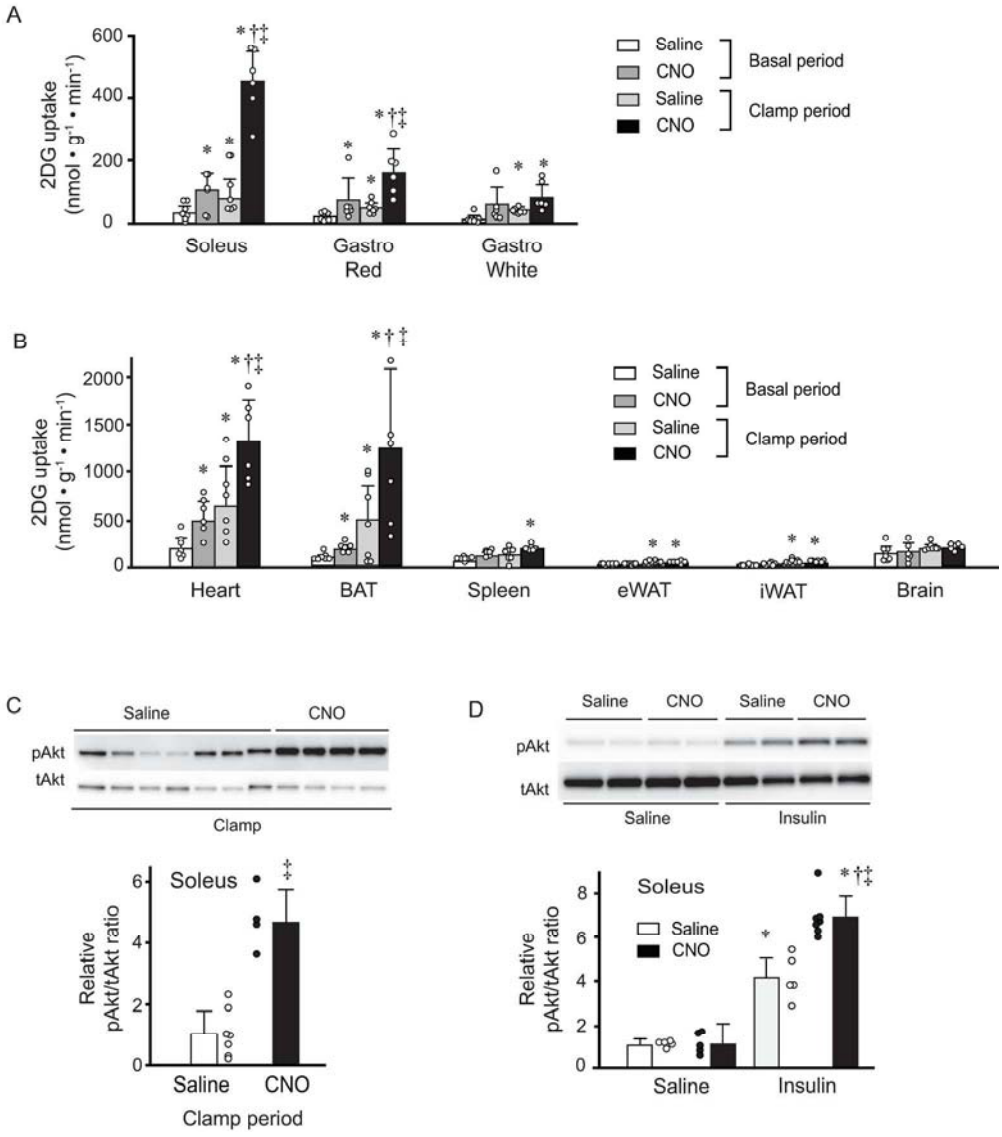

Figure 6

226x267mm (300 x 300 DPI)

Figure 6 (continued)

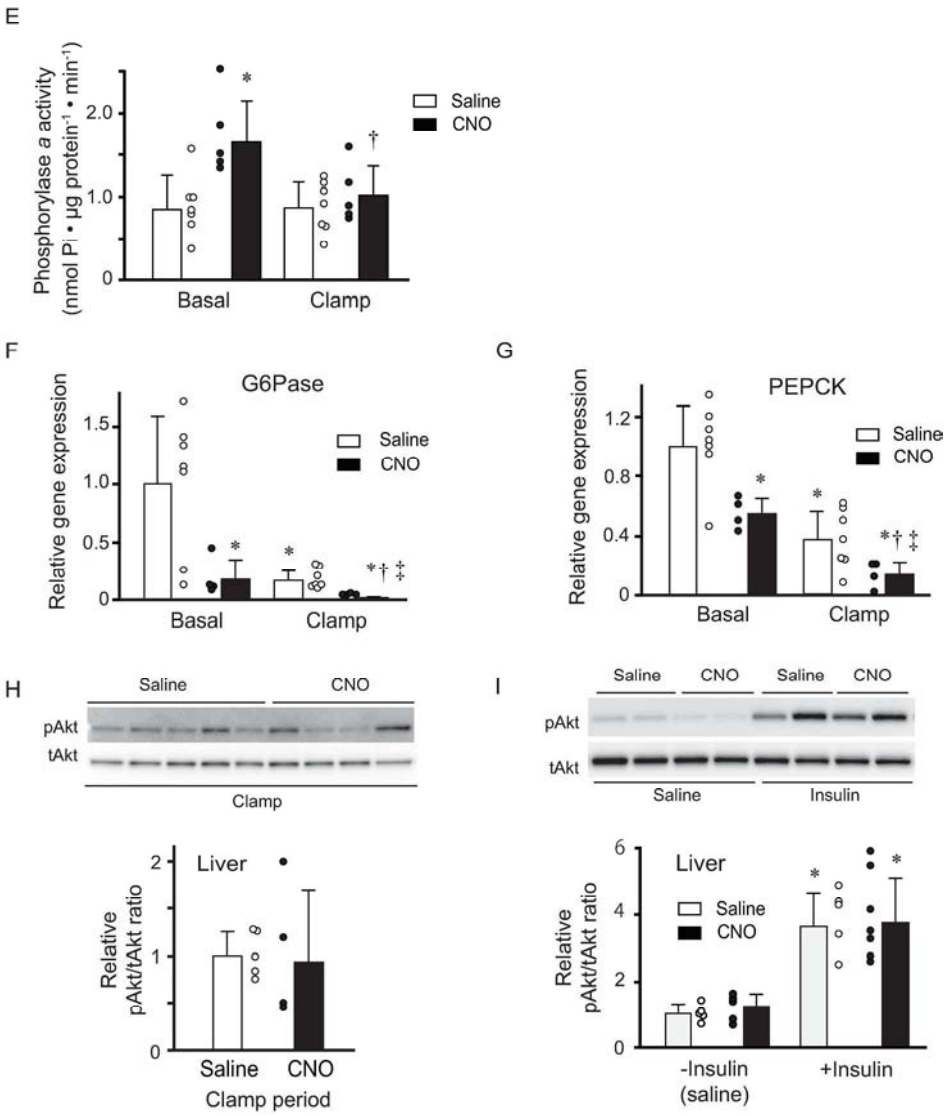

Figure 6 (continued)

220x274mm (300 x 300 DPI)

Supplemental Figure 1

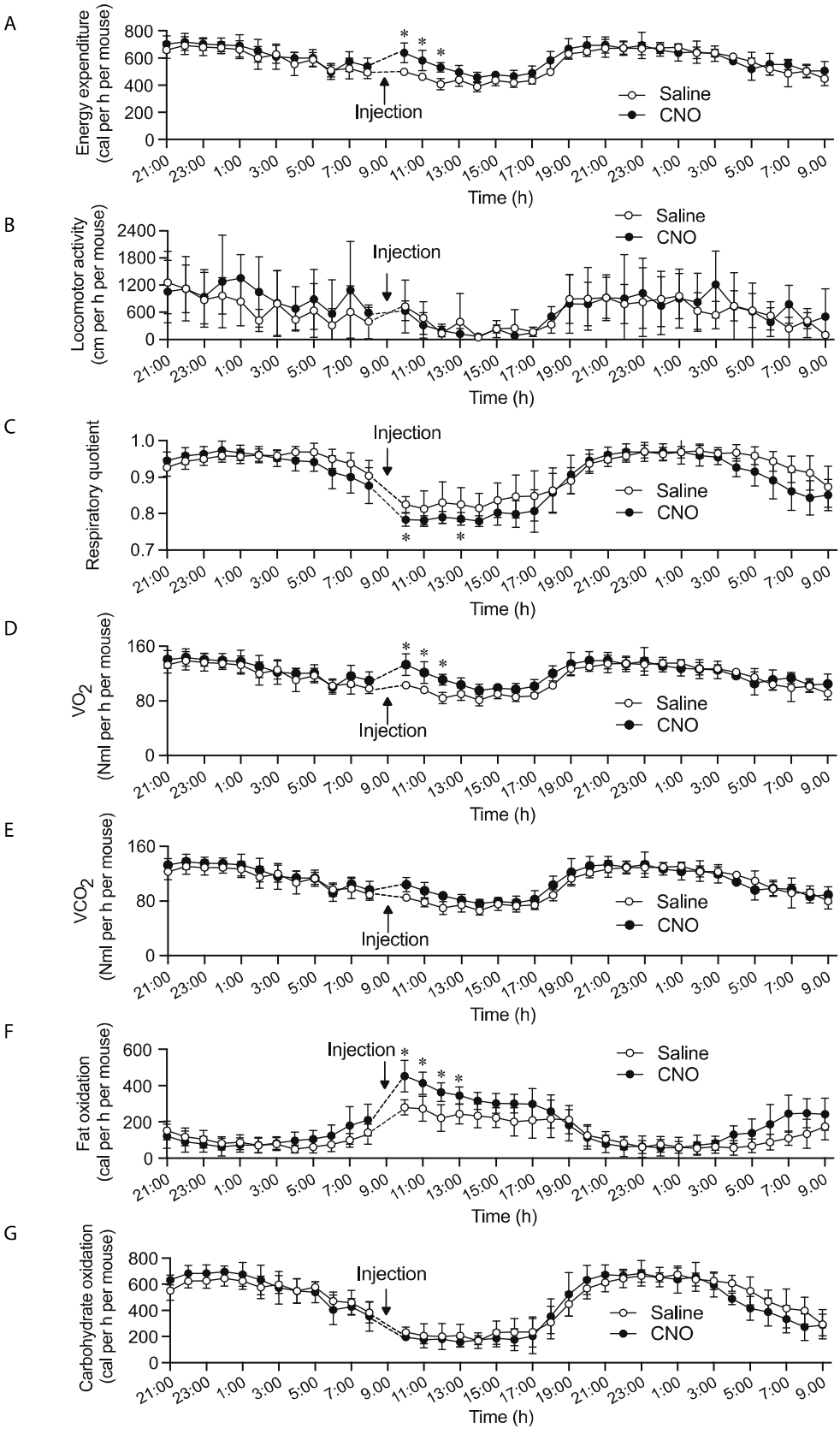

Supplemental Figure 1. Activation of SF1 neurons increases energy expenditure and fat oxidation. Energy expenditure (*A*), locomotor activity (*B*), RQ (*C*), VO_2 (*D*), VCO_2 (*E*), fat oxidation (*F*), and carbohydrate oxidation (*G*) were measured over 36 h. Data are means ± SD (n = 6) and correspond to those shown in Figure 3. *$P < 0.05$ versus corresponding saline value.

Supplemental Figure 2

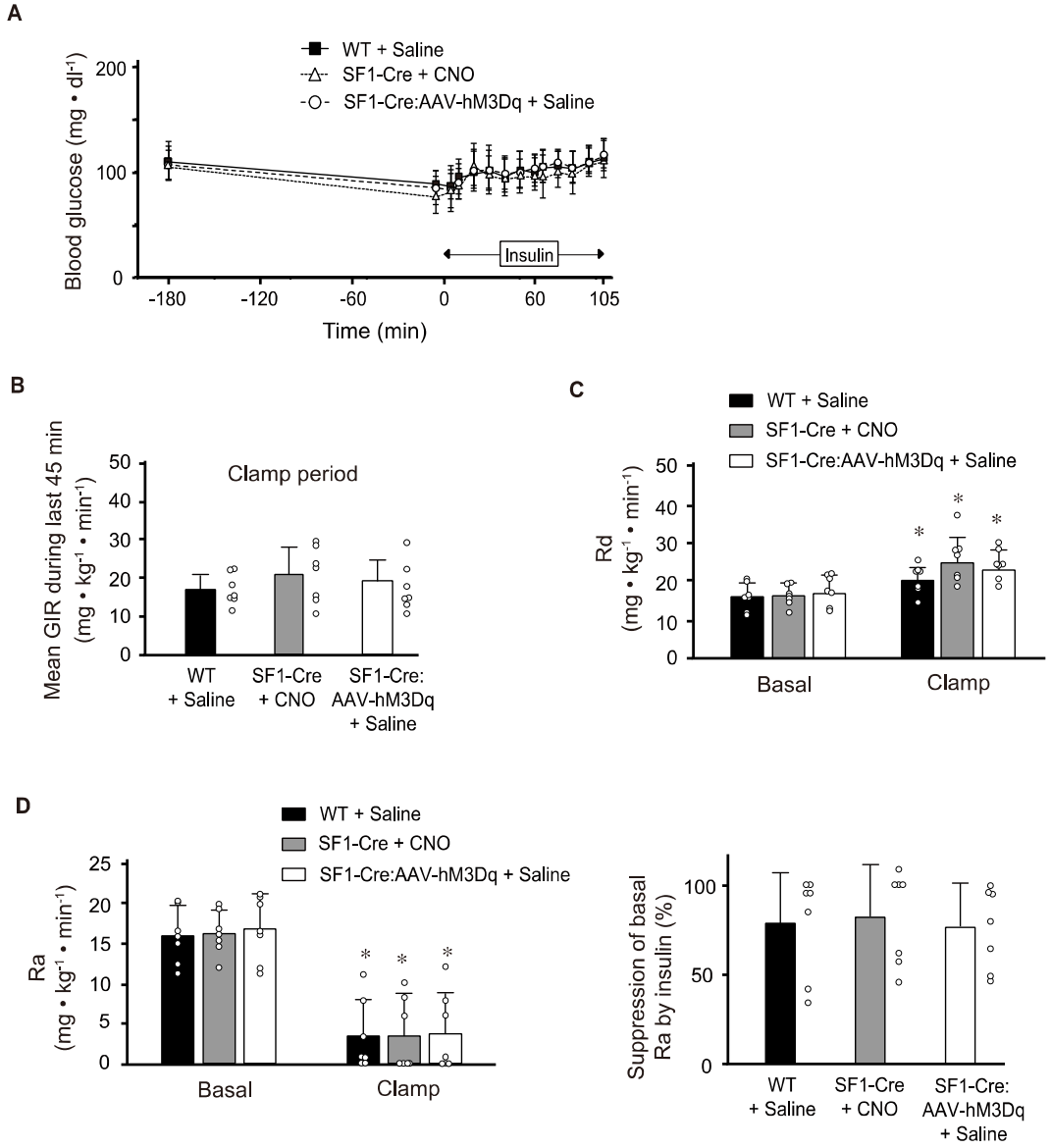

Supplemental Figure 2. No difference in whole-body glucose metabolism among saline-injected WT mice, CNO-injected SF1-Cre mice, and saline-injected SF1-Cre:AAV-hM3Dq mice in the hyperinsulinemic-euglycemic clamp. Blood glucose level (*A*), GIR (*B*), Rd (*C*), as well as Ra and suppression of basal Ra by insulin (*D*) were measured for mice injected intraperitoneally with saline or CNO at t = -180 min. Data for saline-injected SF1-Cre:AAV-hM3Dq mice are the same as those in Figure 5. Data are means ± SD (n = 7). Bar graphs also show the data for individual mice. *P < 0.05 versus corresponding value during basal period.

Supplemental Table

Sequences of PCR primers

Primer	Forward sequence (5'→ 3')	Reverse sequence (3' → 5')
SF1 fwd/ Cre rev (for genotyping)	CTGAGCTGCAGCGCAGGGACA	TGCGAACCTCATCACTCGTTGCAT
Cre recombinase	CTGATTTCGACCAGGTTCGTTC	CGCTCGACCAGTTTAGTTACCC
SF1	GCCAGGAGTTCGTCTGTCTC	ACCTCCACCAGGCACATAG
G3PDH	ACCACAGTCCATGCCATCAC	TCCACCACCCTGTTGCTGTA
G6Pase	CATGGGCGCAGCAGGTGTATACT	CAAGGTAGATCCGGGACAGACAG
PEPCK	GGTGTTTACTGGGAAGGCATC	CAATAATGGGGCACTGGCTG
36B4	GGCCCTGCACTCTCGCTTC	TGCCAGGACGCGCTTGT